Proceedings of the International Conference on Solid-Solid Phase Transformations in Inorganic Materials 2015
Edited by: Matthias Militzer, Gianluigi Botton, Long-Qing Chen, James Howe, Chadwick Sinclair, and Hatem Zurob

PREDICTION OF QUENCHING-INDUCED RESIDUAL STRESS DISTRIBUTION IN 7XXX ALUMINUM ALLOY THICK PLATES USING GLEEBLE INTERRUPTED QUENCH TESTS

N. Chobaut[1], D. Carron[2], P. Schloth[1], S. Arsène[3] and J.-M. Drezet[1]

[1]Ecole Polytechnique Fédérale de Lausanne; station 12, CH-1015 Lausanne, Switzerland
[2]Univ. Bretagne-Sud, EA 4250, LIMATB; F-56100 Lorient, France
[3]Constellium Technology Center; 725 rue Aristide Bergès, Centr'Alp, 38341 Voreppe, France

Keywords: AA7xxx alloys, precipitation, residual stresses, Gleeble machine, neutron diffraction

Abstract

In the fabrication of heat treatable aluminum parts for the aeronautic industry, quenching is a key step to obtain the required mechanical characteristics after aging. For thick plates, thermal gradients cause non-homogeneous plastic strain resulting in residual stresses (RS) after quenching. In 7xxx alloys, precipitation phenomena may affect these RS. Quenching RS are extensively reduced by stress relief. However, RS at final temper could lead to some distortions during machining of large and complex parts. For their prediction, it is thus important to be able to model the full process and particularly the quenching. In this work a simple but realistic approach is presented to predict as-quenched RS. Instead of modeling precipitation, yield strength is characterized with a few Gleeble interrupted quench tests. The results are introduced in a finite element model and predictions are compared to residual stress measurements in plates of different thicknesses for two different 7xxx alloys.

Introduction

In the processing route of heat treatable aluminum alloys (AA), solutionizing and quenching are key steps in order to obtain the required mechanical properties. Ideally, a supersaturated solid solution corresponding to the solid solution after solutionizing and perfect quenching is obtained before aging performed to transform elements in solid solution into fine hardening precipitates and thus increase yield strength. Fast quenching is necessary to avoid coarse precipitation as this one reduces the mechanical properties after heat treatment. However, fast quenching gives birth to high residual stresses (RS). Although these RS in quenched plates are reduced by ~10 after stress relief [1], they could lead in thick 7xxx highly alloyed wrought products to some distortions during machining of large and complex parts at final temper [2].
Precipitation phenomena may affect RS. In 7xxx alloys, two types of precipitation may take place during quenching [3-5]. A first precipitation occurs at intermediate temperature (typically 400-250°C [5]) for low cooling rates. The large precipitates formed are undesirable since they do not harden the material significantly while reducing the amount of elements in solid solution. A second precipitation may occur at low temperature (typically below 300-250°C [5]) even for high cooling rates. In the case of 200 mm thick AA7010 water-quenched plates, the resulting effect of these two types of precipitation is a yield strength increase at the plate surface after quenching [6]. For the prediction of RS, it is thus important to be able to model the full process and particularly the quenching with consideration of potential precipitation phenomena.

Quenching of thick aluminum plates leads to plastic deformation resulting in surface compressive stresses balanced by core tensile stresses after quench [1]. In the particular case of cold-water quenching of thick plates, the surface deforms plastically at high temperature but also at low temperature [6]. The residual stress value at the plate surface depends thus on its yield strength but also on its accumulated inelastic deformation during quenching. The plate mid-thickness area may also deform plastically down to room temperature but less than the surface. At quarter-thickness, the material remains purely elastic.

A thermo-mechanical model ignoring precipitation (TM model) is sufficient to predict satisfactorily as-quenched RS in thin plates where quenching is so fast that precipitation is inhibited and plasticity does not occur at low temperature. In the case of 7xxx highly alloyed thick plates, a TM model underestimates RS since it does not take into account the increase of yield strength by precipitation hardening [7]. The general approach to account for precipitation is to use a thermo-metallurgical-mechanical model based on a yield strength model coupled to a precipitation model [8]. This physically-based model is necessary for modeling complex parts but requires a lot of effort to characterize and model the precipitation of metastable non-stoichiometric phases and clusters during quenching [9, 10].

To avoid such an extensive characterization, an alternative is proposed in this work for modeling cold-water quenching of plates with thicknesses lower than 150 mm of highly alloyed 7xxx alloys. The precipitation-dependent flow stress during quenching is determined *in situ* by Gleeble interrupted quench-tests performed after surface coolings representative of the industrial ones in thick plates and is introduced into a thermo-mechanical model, the so-called TMG model. This simple model does not require a precipitation model, but only a few Gleeble tests for a given alloy and each plate thickness. The RS predicted by the TM model and the TMG model are compared to RS measurements in AA7449 and AA7040 plates of different thicknesses.

Experimental Procedure

20 mm and 75 mm thick AA7449 (Al-7.5–8.7 Zn-1.8–2.7 Mg-1.4–2.1 Cu wt.%) and 75 mm and 140 mm thick AA7040 (Al-5.7–6.7 Zn-1.7–2.4 Mg-1.5–2.3 Cu wt.%) hot-rolled plates were provided by Constellium. For subsequent RS measurements (see details in [7] and [10]), AA7449 and AA7040 plates were vertically quenched by immersion in an experimental medium size agitated 20°C water quench device.

For characterization of material properties during quenching, tensile specimens were taken from quarter-thickness in the rolling direction of the 75 mm hot-rolled AA7449 and AA7040 plates. Samples were presolutionised in a furnace for 4 hours, quenched in cold-water and stored in a freezer at ca. -10°C to retard any precipitation. The Gleeble 3500 machine was selected for its precise temperature control in order to perform interrupted quench-tests [10]. Specimens are heated by Joule effect at 30 K/s to the solutionizing temperature while the force is maintained near zero to allow free dilatation. This high heating rate together with a solutionizing time of 3 min in the Gleeble are chosen to obtain a solid solution at equilibrium, i.e. without any precipitates. For each alloy, one specimen was subjected at the solutionizing temperature to a succession of tensile loads at different strain rates. The other specimens were isothermally tensile tested after being cooled from the solutionizing temperature with either [10]:

- fast quenching in order to characterize the solid solution without precipitates,
- coolings similar to the ones of the surface during quenching (later called “surface coolings”) in order to take into account precipitation in a simple way.

Modeling

Thermo-mechanical model of quenching

The vertical quenching in cold water of AA7449 and AA7040 thick plates was simulated using a pseudo-2D thermo-mechanical model implemented in the commercial finite element (FE) code ABAQUS 6.10. This simple model is fully detailed in Ref. [10]. In this model, only the in-plane components σ_{xx} and σ_{yy} of the stress tensor are different from zero as verified experimentally by layer removal and neutron diffraction [7]. In this model, stress and strain components are 2-D in the plane (plane stress) with:

$$\sigma_{xx}(z) = \sigma_{yy}(z)\ ,\ \sigma_{zx} = \sigma_{zy} = \sigma_{xy} = 0 \text{ and } \sigma_{zz}(z) = 0 \quad (1)$$

where x and y are the in-plane directions and z is the short transverse direction. A non-linear heat transfer analysis is performed using temperature-dependent thermal diffusivity (see Ref. [10]) and heat transfer coefficient determined within the European project COMPACT [11].

Thermo-mechanical behaviour

In order to fit the measured stress-strain curves, an elasto-viscoplastic constitutive model with additive hardening is chosen [10]. Neglecting kinematic hardening (checked on AA7040 by a dedicated experiment [10]), an uniaxial monotonic load at constant temperature is defined by:

$$\sigma_{zz} = \sigma_y + H.(p_{cum})^n + K.(\dot{p})^m \text{ with } \dot{p} = \left|\dot{\varepsilon}_{zz}^{in}\right| \text{ and } p_{cum} = \int_{T<T_{cum}} \dot{p}\ dt \quad (2)$$

where σ_{zz} is the axial flow stress, $\dot{\varepsilon}_{zz}^{in}$ is the inelastic strain-rate and p_{cum} is the accumulated inelastic deformation defined using the parameter T_{cum} corresponding to the temperature above which inelastic deformation has no effect on subsequent low temperature behaviour. This is a simple way to consider plastic strain recovery at high temperature [10]. In Eq. 2, σ_y is the yield strength at 0% strain offset, H and n are hardening parameters, K is the consistency and m is the strain-rate sensitivity parameter. Precipitation mainly affects σ_y, which depends on the size and volume fraction of precipitates as well as on solute concentration in the matrix [8]. The use of Eq. 2, which considers only isotropic hardening, is justified by low plastic strains during quenching (~1%) and the low Bauschinger effect for underaged AA7040 [10] and AA7449 [12].

Results and Discussion

Characterization of material properties during quenching

The imposed temperature cycles are given exemplarily for AA7040 in Figure 1-left and the measured stress-strain curves are shown in Figure 1-right. The fastest quenches are achieved by water quench interrupted at either 100°C or 20°C. Water quench interrupted at higher temperatures was too challenging. Hence, compressed air is used instead above 100°C. This results in lower cooling rates with a risk of precipitation at intermediate temperatures (150-250°C) during air quench. Figure 1-left shows these air quenches for AA7040, which are interrupted at either 440°C, 400°C, 325°C, 265°C, 200°C or 150°C where isothermal tensile loads are performed.

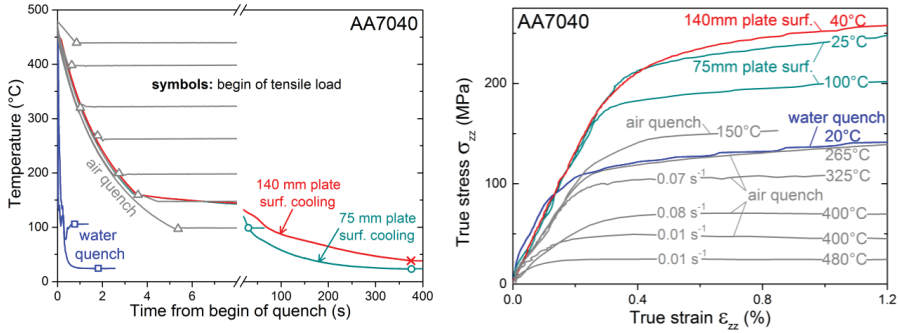

Figure 1. Interrupted quenches (left) achieved with AA7040 Gleeble specimens subjected to tensile loads at constant temperature (right).

The other coolings follow accurately the surface coolings of 75 and 140 mm thick AA7040 plates determined by the heat transfer simulation. These surface coolings are interrupted at either 100°C or 20-40°C to perform tensile loads at constant temperature. At high temperature, the tensile curves feature high strain-rate sensitivity as shown exemplarily for AA7040 at 400°C in Figure 1-right. Strain hardening is negligible above ~350°C. AA7449 also exhibits these two features (not shown). At low temperature, it has been checked that AA7449 and AA7040 exhibit a negligible strain-rate sensitivity below ~300°C (not detailed here), as also shown by Godard [8] for the solid solution behaviour of AA7010. The tensile curves below ~300°C feature some strain hardening that is little affected by the cooling paths as assumed in the model.

Yield strength increases during cooling due to the combined effects of temperature decrease and precipitation. The strength increase from 100°C to 25°C after the 75 mm plate surface cooling is attributed to the formation of hardening clusters at low temperature as observed by *in situ* small angle X-rays scattering (SAXS) during cooling of AA7040 at similar cooling rates to the ones encountered during quenching of thick plates [13]. Similar measurements on AA7449 also revealed cluster formation below 250°C [5].

Using the stress-strain curves after interrupted quench-tests, the five model parameters (σ_y, H, n, K, m) are determined (Figure 2) by inverse method using a dedicated optimization software (SiDoLo) developed by Pilvin [14]. The identification procedure is fully detailed in Ref. [10].

The strain-hardening parameters H and n are highest at low temperature due to maximum dislocation storage and decrease with increasing temperature due to dislocation annihilation. At high temperature ($\geq$ 400°C) where H is set close to zero (Figure 2-a), n is also set close to zero (Figure 2-b) in accordance with Magnin's results [15]. While n is almost identical for AA7040 and AA7449, H is higher for AA7449 than for AA7040. This can be explained by the effect of solute content [16] which is higher in AA7449 than in AA7040.

The K-Temperature curves (Figure 2-a) obtained for AA7449 and AA7040 have a bell-shape typically encountered for metallic alloys [17]. This is explained by low K values at low temperature (< 250°C) where strain-rate sensitivity is small but also low K values at high temperature where the viscous stress is limited by the ultimate strength which becomes small. Below 300°C, m is set to low values and increases rapidly at higher temperatures (Figure 2-b).

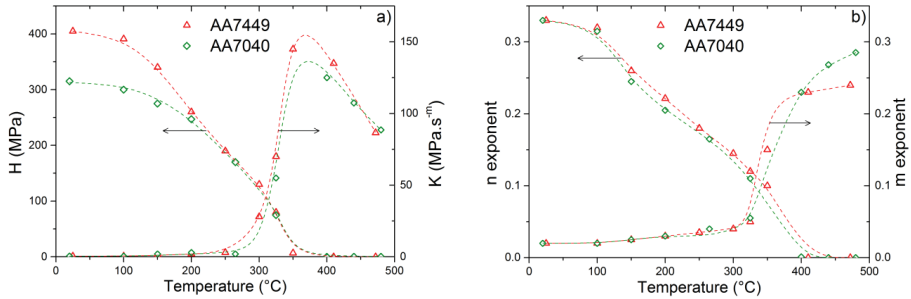

Figure 2. Parameters of Eq. 2 for AA7449 and AA7040. Dashed lines are guides for the eye.

For FE quenching simulations (next section), the temperature-dependent parameters (H, n, K, m) are interpolated linearly as a function of temperature. Moreover, since they are considered independent of precipitation [10], they are treated as uniform material properties (applied through the whole thickness) and the same values are used for both models (TM and TMG).

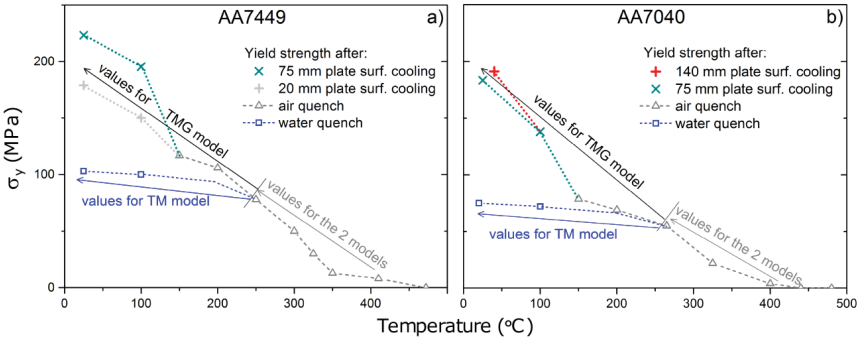

Figure 3. Values of σ_y used for the FE quenching simulations of AA7449 (a) and AA7040 (b) plates using either the TM model or the TMG model.

At high temperature, the same σ_y values (Figure 3) are applied through the whole thickness for the two models since the volume fraction of η phase formed during cold-water quench is low as shown by *in situ* SAXS measurements [13]. In other words, σ_y is considered little affected by high temperature precipitation due to the short time spent at high temperature during quenching. The TM and TMG models differ only from σ_y at low temperature. The TM model and TMG model are fed by σ_y values after fast quenches and after "surface coolings" respectively. The same parameter $\sigma_y(T)$ is applied through the whole thickness and interpolated linearly as a function of temperature. This is a simplification for the TMG model because σ_y should also depend on position through plate thickness since precipitation varies with cooling paths. Nevertheless, as plasticity mainly occurs near the surface for thick plates, σ_y in the model can be considered as temperature-dependent only, provided it is determined through Gleeble interrupted quench-tests after surface coolings. This is a simplified way to account for precipitation. Besides interrupted quench-tests at high temperature, the TMG model requires only two Gleeble tests at

low temperature (25°C and 100°C) where the plate surface plastifies. These tests are performed for each plate thickness and alloy that one wants to model since cooling path depends on these two parameters.

FE simulations of quenching

The RS profiles obtained using the TMG model are given in Figure 4 together with the simulation ignoring precipitation (TM model). RS measurements in both alloys by layer removal and neutron diffraction techniques in the as-quenched state are also shown.

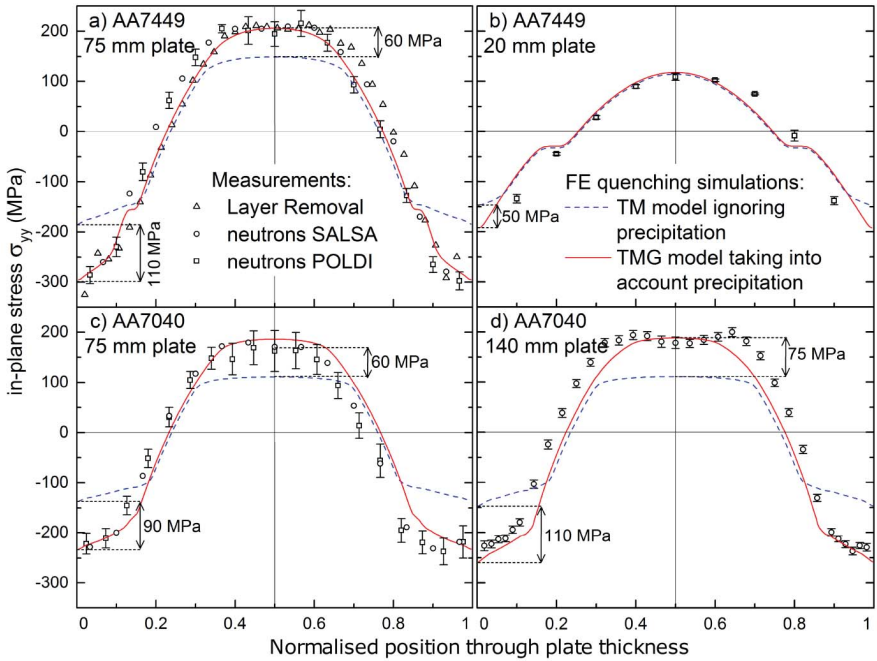

Figure 4. Comparison between measured RS and calculated RS in 75 mm (a) and 20 mm (b) thick AA7449 plates and in 75 mm (c) and 140 mm (d) thick AA7040 plates. The legend of the measurements is given in (a) and the legend of the simulations in (b). T_{cum} = 325°C according to dedicated experiments performed on AA7449 and AA7040 [10].

Except for the 20 mm thick AA7449 plate, the TM model underestimates surface RS because the flow stress in the simulation without precipitation is lower than the real flow stress of the surface. The RS at mid-thickness are also underestimated because the compressive stresses are balanced by tensile stresses through thickness. The TMG model taking into account precipitation predicts very accurately the RS profile in the 75 mm thick plates (solid lines in Figures 4-a and c). For the 140 mm thick AA7040 plate (Figure 4-d), the model with precipitation predicts well the RS at surface and satisfactorily at mid-thickness. In the 20 mm thick AA7449 plate (Figure 4-b), the RS at mid-thickness predicted with or without precipitation compare well with the

measurements. Indeed, the cooling of the 20 mm plate is so fast that precipitation hardening is limited. However, it is not negligible as revealed by the 50 MPa difference between simulations with and without precipitation at the surface. Robinson *et al.* [18] measured ca. 180 MPa compressive stress at the surface of a 16 mm thick AA7010 block. AA7449 containing more alloying elements than AA7010, surface RS in compression should be higher than 180 MPa in a 20 mm thick AA7449 plate. This is in accordance with the 200 MPa compressive stresses predicted by the simulation with the TMG model.
The RS underestimation by the TM model without precipitation increases with increasing thickness. Thus, the thicker the plate is, the more important it is to use a model with precipitation, which predicts reasonably well the RS profile.
The good agreement between the TMG model taking into account precipitation and the measurements shows the relevance of a model based on tensile tests after cooling similar to the one of the surface during quenching. But it means that a few Gleeble tensile tests should be performed for each plate thickness and each alloy one would like to model, namely:

- for each alloy, one tensile test at the solutionizing temperature and a few tensile tests after rapid cooling between the solutionizing temperature and 200°C,
- for each alloy and plate thickness, two tensile tests at lower temperature (e.g. 25°C and 100°C) after a cooling similar to the one of the surface during quenching.

The advantage of the present model resides in the limited number of Gleeble tests compared to the traditional approach based on a yield strength model depending on precipitation. Indeed such an approach requires a lot of effort to characterize and simulate the precipitation of metastable non-stoichiometric phases and GP zones during quenching.

Conclusion

A simple but realistic approach is presented to predict residual stress in thick AA7xxx plates. High temperature isothermal tensile tests were achieved for each alloy after fast quench. Yield strength values were also measured after surface coolings for each plate thickness and each alloy and then introduced in a FE model to predict through thickness residual stresses. This simple approach takes into account the influence of precipitation hardening on the increase of surface RS and is tested for three plate thicknesses and two different 7xxx alloys. The agreement between measured and simulated residual stresses is excellent. Compared to a more sophisticated thermo-metallurgical-mechanical model, the present approach decreases the number of Gleeble tests and does not require a complete characterization of precipitation.

Acknowledgements

This work is funded by the Competence Center for Materials Science and Technology in the frame of the project entitled “Measurements and modeling of residual stress during quenching of thick heat treatable aluminum components in relation to their microstructure” involving EPF Lausanne, PSI Villigen, Univ. Bretagne-Sud Lorient, Constellium and ABB Turbo Systems Ltd. The Gleeble 3500 machine of Université de Bretagne-Sud was co-financed by European Regional Development Fund. The authors are indebted to the Institut Laue-Langevin in France and the Swiss Spallation Neutron Source in Switzerland for neutron beam time. The authors are grateful to Prof. P. Pilvin for providing SiDoLo, J. Costa and W. Berckmans (Univ. Bretagne-Sud) for the instrumentation of the Gleeble specimens.

References

[1] J.C. Boyer and M. Boivin, "Numerical calculations of residual-stress relaxation in quenched plates", *Materials Science and Technology*, 1 (10) (1985), 786-792.

[2] B. Dubost et al., "Prediction and Minimization of Residual Stresses in Quenched Aluminium Alloy Die Forgings", *Proceedings of the International Conference on Residual Stresses, Edited by: G. Beck, S. Denis and A. Simon, Springer*, (1989), 581-586.

[3] D. Dumont et al., "Characterisation of precipitation microstructures in aluminium alloys 7040 and 7050 and their relationship to mechanical behaviour ", *Materials Science and Technology*, 20 (5) (2004), 567-576.

[4] D. Godard et al., "Precipitation sequences during quenching of the AA 7010 alloy", *Acta Materialia*, 50 (9) (2002), 2319-2329.

[5] P. Schloth et al., "Early precipitation during cooling of an Al-Zn-Mg-Cu alloy revealed by in situ small angle X-ray scattering", *Applied Physics Letters*, 105 (10) (2014), 101908.

[6] D. Godard et al., "Modelling of heat treatment residual stresses. Application to high strength aluminium alloys including precipitation effects", *Proceedings of the 7th International Seminar of IFHT on Heat Treatment and Surface Engineering of Light Alloys, Edited by: J. Lendvai and T. Réti*, (1999), 249-257.

[7] N. Chobaut et al., "Residual stress analysis in AA7449 as-quenched thick plates using neutrons and FE modelling", *Proceedings of ICAA13, Edited by: Hasso Weiland, Anthony D. Rollett, William A. Cassada, TMS*, (2012), 285–291.

[8] D. Godard, "Influences de la précipitation sur le comportement thermomécanique lors de la trempe d'un alliage Al-Zn-Mg-Cu" (Ph.D. thesis, INPL, 1999).

[9] D. Godard et al., "Mechanical softening kinetics at high temperatures in AlMgZnCu Alloy: experimental characterization and microstructural interpretation", *Proceedings of ICAA6, Edited by: T. Sato, S. Kumai, T. Kobayashi, Y. Murakami*, (1998), 1033-1038.

[10] N. Chobaut, "Measurements and modelling of residual stresses during quenching of thick heat treatable aluminium components in relation to their precipitation state" (Ph.D. thesis 6559, EPFL, 2015).

[11] X. Yu and J.S. Robinson, "Measurement of the heat transfer coefficient during quenching of the aluminium alloy 7449" (*COMPACT project report*, 2007).

[12] G. Fribourg et al., "Microstructure-based modelling of isotropic and kinematic strain hardening in a precipitation-hardened aluminium alloy", *Acta Materialia*, 59 (9) (2011), 3621-3635.

[13] P. Schloth, "Precipitation in the high strength AA7449 Aluminium alloy: implications on internal stresses on different length scales" (Ph.D. thesis 6525, EPFL, 2015).

[14] P. Pilvin and G. Cailletaud, "Identification and inverse problems related to material behaviour", *Proceedings of the second International Symposium on Inverse Problems, Edited by: H.D. Bui, M. Tanaka, M. Bonnet, H. Maigre, E. Luzzato and M. Reynier, Balkema*, (1994), 79–86.

[15] B. Magnin et al., "Ductility and rheology of an Al-4.5% Cu alloy from room temperature to coherency temperature", *Materials Science Forum*, 217 (1996), 1209-1214.

[16] J.P. Suni et al., "Solute dependence of cold work strengthening in aluminium alloys", *Proceedings of ICAA4*, 1 (1994), 521-528.

[17] B. Barlas, "Etude du comportement et de l'endommagement en fatigue d'alliages d'aluminium de fonderie" (Ph.D. thesis, Ecole des Mines de Paris, 2004).

[18] J.S. Robinson et al., "50th Anniversary Article: The Origin and Management of Residual Stress in Heat-treatable Aluminium Alloys", *Strain*, 50 (3) (2014), 185-207.